atmosphere

MDPI

*Article*

# $PM_{10}$ Element Distribution and Environmental-Sanitary Risk Analysis in Two Italian Industrial Cities

**Aleandro Diana [1], Stefano Bertinetti [1,*], Ornella Abollino [2], Agnese Giacomino [2], Sandro Buoso [1], Laura Favilli [2], Paolo Inaudi [2] and Mery Malandrino [1,*]**

[1] Department of Chemistry, University of Turin, 10125 Turin, Italy
[2] Department of Drug Science and Technology, University of Turin, 10125 Turin, Italy
* Correspondence: stefano.bertinetti@unito.it (S.B.); mery.malandrino@unito.it (M.M.)

**Abstract:** In this work, an evaluation of the air of two Italian industrial cities, Turin and Biella, has been performed to identify the main sources affecting its quality and to evaluate its evolution along 15 years. These two cities are placed at the border of the Po valley, one of the most polluted areas of Europe, and the automotive and textile industries have been their main economic sectors. The elemental analysis of the $PM_{10}$ collected there in 2007 has been performed by ICP-MS and ICP-AES. The results identify the urban activities and the soil/road dust resuspension as the main sources of metals. Biella was overall less polluted in $PM_{10}$ than Turin, probably because of its smaller size, its smaller traffic volume, and the lower number of industries. However, the limit value imposed by the European legislation for daily average $PM_{10}$ mass concentration (50 μg $m^{-3}$) was frequently exceeded in the collected samples: 22% and 50%, respectively for Biella and Turin. The concentration of specific toxic metals regulated by Italian legislation was never higher than the limit value for Cd (4 ng $m^{-3}$) and Pb (0.5 μg $m^{-3}$), whereas it was exceeded for Ni (20 ng $m^{-3}$) in 22% of the samples from Turin and only in the 5% of those from Biella. In the same way, the risk analysis, performed using the target hazard quotient (THQ), calculated for children and adult populations, did not reveal warning values. Only for Cd in children were concerning values found (median THQ = 4.9). Element concentrations showed a seasonal trend, with higher values in November and December due to a combination of stable atmospheric conditions and strengthening of anthropic sources (e.g., combustion for heat generation). Finally, data concerning the amount of Cd, Ni, and Pb in the atmosphere provided by the regional agency for environmental protection (ARPA Piedmont) have been used to follow the evolution of these elements from 2007 to 2021 in the two cities. The data reveal a significant reduction of the concentrations of all considered metals in all the sites (higher than 50%), however maintaining the seasonal variability observed in $PM_{10}$ samples of 2007, with higher concentrations during the cold months and lower concentrations during the summer.

**Keywords:** particulate matter; urban air pollution; element distribution; Target Hazard Quozient (THQ); chemometric elaboration



**Citation:** Diana, A.; Bertinetti, S.; Abollino, O.; Giacomino, A.; Buoso, S.; Favilli, L.; Inaudi, P.; Malandrino, M. $PM_{10}$ Element Distribution and Environmental-Sanitary Risk Analysis in Two Italian Industrial Cities. *Atmosphere* **2023**, *14*, 48. https://doi.org/10.3390/atmos14010048

Academic Editors: Nima Afshar-Mohajer and Sinan Sousan

Received: 1 December 2022
Revised: 19 December 2022
Accepted: 23 December 2022
Published: 27 December 2022



## 1. Introduction

Aerosol air pollution is a major world concern, mainly due to its effects on atmospheric chemistry, the hydrological cycle and climate, as well as public health [1–3]. Despite improvements in the last decades, atmospheric particulate matter (PM) is still a major health concern for Europeans [4]. According to the World Health Organization (WHO), every year, exposure to air pollution is estimated to cause 7 million premature deaths and result in the loss of millions more healthy years of life [5]. In 2019, air pollution continued to drive a significant burden of premature death and disease in Europe even if, compared to 2005, premature deaths attributed to exposure to fine particulate matter decreased by 33% in the 27 Member States of the European Union [4].

$PM_{10}$ (aerodynamic equivalent diameter lower than 10 μm) fraction is studied as carrier of many harmful trace elements (such as As, Cd, Cr, Cu, Hg, Mn, Ni, Pb, Se, V, and Zn) into the human respiratory system [6–8]. The association between PM and adverse health effects [9,10] led to Directive 2008/50/CE [11] and to Directive 2004/107/CE [12], which determined specific target values for the presence of $PM_{10}$ (50 μg $m^{-3}$), $PM_{2.5}$ (25 μg $m^{-3}$ and 20 μg $m^{-3}$, from 2020) and the concentrations of several chemical elements, namely arsenic (6 ng $m^{-3}$), cadmium (5 ng $m^{-3}$), nickel (20 ng $m^{-3}$), and lead (0.5 μg $m^{-3}$), in $PM_{10}$ (Italian transposition of Directive: D. Lgs. 155, 2010 [13]). Since toxic and carcinogenic properties are well known for many metals, the environmental-sanitary risk assessment has assumed a central role in the evaluation of the urban air quality in order to estimate if the metals in the $PM_{10}$ may pose a health risk to children or adults via inhalation of airborne PM [8,14,15].

The Po Valley covers the territory of several regions in Northern Italy and includes many urban agglomerates, such as Turin, Biella, Milan, Venice, and Bologna. The area is densely populated and heavily industrialized. High amounts of atmospheric pollutants are emitted per year by a wide variety of pollution sources, which are mainly related to traffic, domestic heating, industry and energy production, agriculture, and farming activities [16]. Furthermore, the geographic conformation of the valley prevents an efficient dispersion of primary pollutants and causes a consequent high formation of secondary pollutants, making this study area subject to public health consideration [17]. The European Environmental Agency confirmed the Po Valley as a hot spot region for air pollutants in their 2021 report [4].

In the past, Turin and Biella (Piedmont, Italy, Figure 1) were two heavily industrialized cities, mainly for the automotive and textile industries respectively. From this, it follows that air pollution was mainly determined by industrial emissions. To date, both cities are mostly dedicated to tourism and commercial activities, even if industrial activities are still present, especially in the metropolitan area of Turin. Moreover, in the last fifteen years, there has been an impressive increase in the demand for mobility which has led to a progressive and significant change in the modal ratio of transport flows, in favor of road transport for both national and regional mobility. This is in accordance with the information reported by the Italian environmental agencies indicating that the low air quality in Italian cities is mainly linked to the number of vehicles per inhabitant: in fact, 670 passenger cars for thousand inhabitants (against the 560 European average) put Italy at the top of world motorization [18].

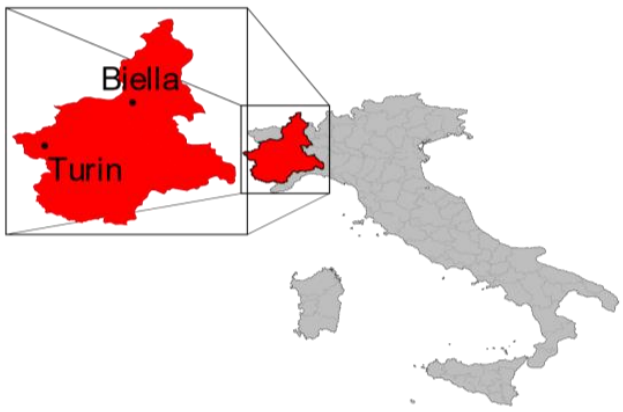


**Figure 1.** Map of Italy. In the magnifying lens is reported the region Piedmont with the geographical position of the cities of Turin and Biella.

Studies of the metal composition of different fractions of PM collected in the urban district of Turin have been previously performed [8,19]. In this study, we determined Ba, Cd, Co, Cr, Cu, Fe, Hg, K, Mn, Mo, Ni, Pb, Si, Ti, V, Zn, and Zr levels in airborne $PM_{10}$ samples collected in Turin and Biella in 2007, when these two cities were characterized by diverse

industrial areas and districts. We calculated enrichment factors (EFs) and applied the most common chemometric techniques (principal component analysis (PCA) and hierarchical cluster analysis (HCA)) to identify and characterize the emission sources influencing $PM_{10}$ in these two typical industrial cities. Moreover, an environmental-sanitary risk assessment was carried out, in order to evaluate if the metals in the $PM_{10}$ could pose a health risk to children or adults via the inhalation of airborne $PM_{10}$. Finally, Cd, Ni, and Pb levels in the $PM_{10}$ collected in the two cities have been used to follow the evolution of these elements from 2007 to 2021 and evidence the effect of the deindustrialization that occurred in the investigated areas, especially following the economic crisis of 2008.

## 2. Materials and Methods

### *2.1. Sampling*

The samples analyzed in this work are part of the continuous $PM_{10}$ monitoring program carried out by the Piedmont Region through the ARPA (Regional Agency for Environmental Protection) at fixed sampling stations. The $PM_{10}$ samples derive from three sampling points: two in the city of Turin (referred to as Consolata site and Grassi site) and one in the city of Biella (referred to as Biella site). All the sampling locations fall into the "urban traffic" station category. The Consolata site is in the center of Turin in a residential and commercial area, mainly affected by vehicular traffic and heating emissions. Grassi site, instead, is in the northern part of the town, in an area characterized by higher vehicular traffic flow and is subjected to various industrial emissions (foundries, automotive, plastic material stamping, etc.). Biella site is mainly affected by vehicular traffic and heating emissions but to a lesser extent in respect of Turin while in the past it was more influenced by the emissions deriving from the textile industries present in the area. The exceedance of daily average $PM_{10}$ mass concentration limit (50 $\mu g\ m^{-3}$) in 2007 was 190, 146, and 73 for Grassi site, Consolata site, and Biella site, respectively [20].

$PM_{10}$ was collected in the sampling stations considered over 24 hours on quartz fibre filters with a diameter of 47 mm, using a gravimetric sampler (according to the standards EN 12341 and DM 60/02).

The device equipment (Skypost PM FX) has a geometry that allows particles with an aerodynamic diameter less than 10 µm to reach the filter. A special system allows the sequential replacement of the exposed filters without interrupting the sampling in progress.

Filters were conditioned before and after sampling for 48 hours at a temperature of $20 \pm 1\ ^{\circ}C$ and controlled humidity at $50 \pm 5\%$. Filters were weighed with an analytical balance and the amount of particulate deposited is calculated from the difference in the filter mass before and after sampling.

### *2.2. Sample Treatment and Analysis*

A total of 107 $PM_{10}$ samples were analyzed: 33 filters from Consolata site, 33 from Grassi site, and 41 from the Biella site. The samples were collected during the months of April, July, November, and December, and only for the Biella site also in August. In this study, we wanted to assess both the possible presence of a seasonal trend for certain elements, as well as the influence of mass concentration on the level of polluting elements in $PM_{10}$. To fulfill the second purpose, it was decided to choose samples with the highest and lowest mass concentrations in the same month.

Acid digestion, performed with a microwave digestion unit (Milestone MLS-1200 Mega), was chosen as $PM_{10}$ dissolution procedure. The filters were cut into two parts, which were separately weighed and treated, using a mixture of 3 ml of sub-boiling $HNO_3$ (prepared from commercial 65% $HNO_3$, Fluka) and 3 ml of $H_2O_2$ (30%, Merck) in PTFE bombs.

Care was taken when handling the filters to avoid contamination: nitrile gloves, plastic tweezers and scissors were always used.

The digestion program consisted of 5 heating steps of 5 min each, except for the first one that lasts 1 min (at 250, 200, 350, 550, and 250 W respectively). Resulting solutions were

filtered on cellulose filters (Albet) and diluted to 30 ml with Milli-Q (Millipore) ultrapure water (18.2 MΩ/cm).

The following analytes were determined: Ba, Cd, Co, Cr, Cu, Fe, Hg, K, Mn, Mo, Ni, Pb, Si, Ti, V, Zn, and Zr. The metal contents were determined using Varian-Liberty 100 ICP-AES and Thermo-Finnigan Element 2 high-resolution ICP-MS (HR-ICP-MS) according to the range of concentrations and instrument sensitivity.

Wavelength, mass resolution, and isotope were selected for each element to ensure the removal of spectral interferences and maximize sensitivity. NIST SRM 1649a (Urban Dust) and BCR 176 (City Waste Incinerator Ash) were used to verify the accuracy of the analytical method: element recovery was always better than 70%, excluding Cr which was better than 50% (Table S1 from Supplementary Materials).

The quantitative determination of the elements was performed by the external calibration method using standard solutions prepared in aliquots of process blanks. Where necessary, Te was used as an internal standard. Sets of instrumental blank and calibration verification checks were run at frequent intervals during the batch sequences for both HR-ICP-MS and ICP-AES analyses.

### *2.3. Chemometric Analysis*

A statistical-chemometric analysis was performed to identify the principal sources of contaminants in the $PM_{10}$, highlighting similitudes and differences in the samples as a function of origin (sampling site) and time (seasonality). Among the available techniques for extracting information from a multivariate dataset, principal component analysis (PCA) and hierarchical cluster analysis (HCA) were used.

PCA allows representing data from multivariate space with a lower number of new variables, called principal components, which are formed by the linear combination of the original ones. The components are sorted according to the fraction of explained variance of the data, which is synonymous of information. Therefore, the first components bring most of the useful information, excluding noise and spurious ones. By the PCA, it is possible to study the relationship between the samples and to highlight the variables that affect the observed relationship [21].

HCA can be used to confirm the groups of variables and samples obtained by PCA, but also identify groups not well detectable with the latter, since HCA considers all the information contained in the dataset. The method groups data by similarity: objects (samples in R-mode and variables in Q-mode) with the maximum similarity are iteratively arranged into groups, or clusters, more and more populous until all objects are in the same group [22].

Data elaboration was performed in the statistical environment R [23] using the toolbox CAT (Chemiometric Agile Tool, [24]) and the packages *ggdendro* [25] and *dendextend* [26].

### *2.4. Risk Analysis*

The harmfulness of $PM_{10}$ is due to the dimension of the particles and to their composition. To evaluate the potential toxicity of the $PM_{10}$ collected in Turin and Biella in 2007, a risk analysis was performed. The receptors considered were adults and children, while the source of contamination was the $PM_{10}$ collected in the two cities in April, July, August, November, and December of 2007. The metals considered for the risk analysis were V, Cr, Mn, Co, Ni, and Cd. In this work, only the inhalation of the $PM_{10}$ was considered as a possible route of contamination. According to USEPA methods for non-carcinogenic chemicals, the target hazard quotient ($THQ$) has been calculated as reported in Equation (1) [8]:

$$THQ = \frac{ADI}{RfDi} \quad (1)$$

where $ADI$, average daily intake, is the estimated dose that the receptor is exposed to from an exposure route; $RfDi$, reference concentration, is the dose for a specific route that is without negative effects. Values of $THQ$ higher than unity indicate a great level of concern

because the dose that the receptor is exposed to is higher than that considered safe. The $RfDi$ values were derived from USEPA reference concentrations ($RfC$), the inhalation rate ($IR$), the absorption rate ($AR$: 100%), and the body weight of receptor ($BW$: 70 Kg and 15 Kg for adults and children, respectively):

$$RfDi = \frac{RfC \times IR \times AR}{BW \times 100} \quad (2)$$

The daily intake $ADI$ is calculated as the product of the specific exposition rate, $E$ ($m^3$ $Kg^{-1}$ $d^{-1}$), and the concentration of the metal ($C$, mg $m^{-3}$):

$$ADI = E \times C \quad (3)$$

$$E = \frac{IR \times ET \times EF \times ED}{BW \times AT} \quad (4)$$

where $ET$ (exposure time) and $EF$ (exposure frequency) were assumed to be equal to 5 h $d^{-1}$ and 350 d $year^{-1}$ both for children and adults, respectively, and $ED$ (exposure duration) was assumed to be equal to 6 years for children and 24 years for adults.

Table 1 reports the values of the parameters utilized to calculate the $RfDi$ values for the considered metals. The assumption that the concentration of metals in the $PM_{10}$ is the same as that found at the receptor was taken, even if it is clearly not correct. Moreover, the parameters utilized for the calculation of the specific rates of exposure were highly conservative.

**Table 1.** $RfC$ data from USEPA database. $RfDi$ values were calculated according to equation (2), using the reported values of $IR$ and $BW$ for adults and children. Standard default exposure factors were used, taking into account the "inhalation of contaminant" as the exposure pathway in a "residential scenario" related to adults and children (male and female combined), for sedentary and light activity [27–29].

| | V | Cr | Mn | Co | Ni | Cd |
|---|---|---|---|---|---|---|
| $RfC$ (mg $m^{-3}$) | $1.0 \times 10^{-4}$ | $1.4 \times 10^{-4}$ | $5.0 \times 10^{-5}$ | $6.0 \times 10^{-6}$ | $9.0 \times 10^{-5}$ | $1.0 \times 10^{-5}$ |
| $RfCi$ (mg $Kg^{-1}$ $d^{-1}$) | $2.86 \times 10^{-5}$ | $4.00 \times 10^{-5}$ | $1.43 \times 10^{-5}$ | $1.71 \times 10^{-6}$ | $2.57 \times 10^{-5}$ | $2.86 \times 10^{-6}$ |
| $IR$ (adult, $m^3$ $h^{-1}$) | 0.9 | 0.9 | 0.9 | 0.9 | 0.9 | 0.9 |
| $IR$ (children, $m^3$ $h^{-1}$) | 0.7 | 0.7 | 0.7 | 0.7 | 0.7 | 0.7 |
| $BW$ (adult, Kg) | 70 | 70 | 70 | 70 | 70 | 70 |
| $BW$ (children, Kg) | 15 | 15 | 15 | 15 | 15 | 15 |

## 3. Results and Discussion

### 3.1. $PM_{10}$ and Metal Concentrations

Figure 2 shows the concentrations of $PM_{10}$ for each sample analyzed in the three investigated sites, expressed in $\mu g/m^3$.

$PM_{10}$ trends are similar in all the sites investigated. High concentrations of $PM_{10}$ can be noticed in November and December samples with maximum values of 174 μg $m^{-3}$ for sample G 07_12 (Grassi site), 127 μg $m^{-3}$ for sample C 20_11 (Consolata site), 80 μg $m^{-3}$ in B 02_12 (Biella site). Indeed, in these months we noticed the most frequent overcomes of the daily value of 50 μg $m^{-3}$, especially for Turin sites: 12 out of 15 for the Grassi site, 10 out of 14 for the Consolata site, whereas for the Biella site we had six out of 15 overcomes.

These results confirmed how in the cold months the contributions of emissions from vehicular traffic, heating and industrial plants combine with the most unfavorable atmospheric conditions (e.g., strong thermal inversion) to promote the accumulation of pollutants in the low troposphere [30,31].

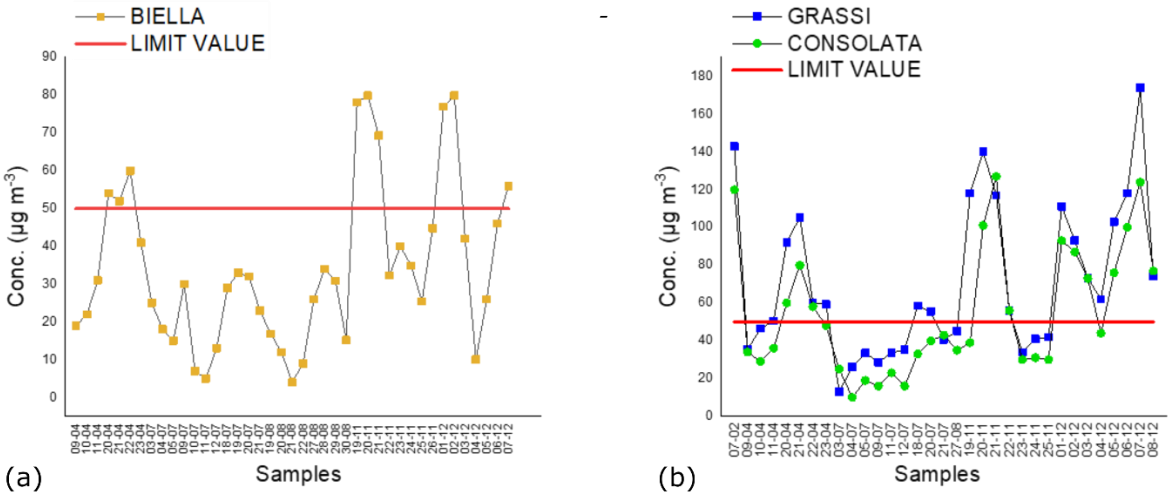


**Figure 2.** Concentrations of $PM_{10}$ samples expressed in µg $m^{-3}$ for (**a**) Biella site and (**b**) sites of Turin (Grassi and Consolata). The red lines indicate the law limit of 50 µg $m^{-3}$.

The lowest $PM_{10}$ concentrations are in July and August with values of 13 µg $m^{-3}$ in G 03_07, 10 µg $m^{-3}$ in C 05_07 and 4 µg $m^{-3}$ in B 21_08.

In the summer season, the contribution of emissions from heating plants is not present and, in addition, more unstable weather conditions occur with an increase in rainfall and windiness, leading to a minor content and residential time of $PM_{10}$ in the low troposphere.

This seasonal trend has also been highlighted by other studies made in the area of the Po valley [32–34].

Tables 2–4 show average, minimum, maximum, 5° percentile, and 95° percentile concentrations expressed in ng $m^{-3}$ for each element determined in the $PM_{10}$ samples from Biella site, Consolata site, and Grassi site, respectively.

**Table 2.** Concentrations of mean, minimum, maximum, 5th percentile, 95th percentile of the analytes determined, expressed in ng $m^{-3}$, for Biella site.

| | Mean | Min | Max | 5th Percentile | 95th Percentile |
|---|---|---|---|---|---|
| K | 203 | 55 | 586 | 157 | 484 |
| Ti | 12 | 2 | 39 | 10 | 31 |
| V | 5 | 0.7 | 12 | 4 | 11 |
| Cr | 3 | 0.2 | 10 | 3 | 7 |
| Mn | 8 | 1 | 24 | 6 | 20 |
| Fe | 322 | 63 | 1069 | 215 | 793 |
| Co | 0.5 | 0.02 | 2.4 | 0.2 | 2.0 |
| Ni | 8 | 2 | 21 | 7 | 20 |
| Cu | 12 | 1 | 43 | 9 | 29 |
| Zn | 33 | 9 | 107 | 25 | 93 |
| Cd | 0.4 | 0.1 | 2.7 | 0.3 | 0.6 |
| Ba | 29 | 2 | 84 | 22 | 77 |
| Hg | 1 | 0.3 | 5 | 1 | 4 |
| Pb | 9 | 1 | 36 | 4 | 31 |
| Mo | 1 | 0.2 | 5 | 0.6 | 3 |
| Si | 1692 | 253 | 6810 | 418 | 3876 |
| Zr | 0.2 | 0.03 | 0.7 | 0.2 | 0.6 |

**Table 3.** Concentrations of mean, minimum, maximum, 5th percentile, 95th percentile of the analytes determined, expressed in ng $m^{-3}$, for Consolata site.

| | Mean | Min | Max | 5th Percentile | 95th Percentile |
|---|---|---|---|---|---|
| K | 555 | 42 | 2340 | 410 | 1815 |
| Ti | 22 | 4 | 48 | 18 | 41 |
| V | 5 | 0.9 | 15 | 5 | 10 |
| Cr | 11 | 0.2 | 32 | 9 | 28 |
| Mn | 24 | 6 | 71 | 21 | 52 |
| Fe | 1430 | 588 | 3863 | 1200 | 3256 |
| Co | 0.7 | 0.3 | 2.3 | 0.5 | 1.6 |
| Ni | 16 | 0.6 | 198 | 8 | 28 |
| Cu | 73 | 30 | 212 | 60 | 179 |
| Zn | 89 | 24 | 253 | 78 | 163 |
| Cd | 0.8 | 0.2 | 4.0 | 0.8 | 1.4 |
| Ba | 72 | 9 | 146 | 81 | 114 |
| Hg | 3 | 1 | 11 | 2 | 10 |
| Pb | 20 | 6 | 73 | 15 | 53 |
| Mo | 5 | 2 | 13 | 4 | 10 |
| Si | 3437 | 1418 | 5667 | 3294 | 5277 |
| Zr | 1.4 | 0.6 | 3.8 | 1.3 | 2.4 |

**Table 4.** Concentrations of mean, minimum, maximum, 5th percentile, 95th percentile of the analytes determined, expressed in ng $m^{-3}$, for Grassi site.

| | Mean | Min | Max | 5th Percentile | 95th Percentile |
|---|---|---|---|---|---|
| K | 947 | 151 | 8715 | 582 | 2823 |
| Ti | 32 | 7 | 77 | 28 | 64 |
| V | 5 | 2 | 12 | 4 | 9 |
| Cr | 15 | 2 | 48 | 12 | 42 |
| Mn | 34 | 7 | 95 | 29 | 75 |
| Fe | 2079 | 113 | 5827 | 1872 | 4532 |
| Co | 0.6 | 0.08 | 2.5 | 0.5 | 1.8 |
| Ni | 20 | 3 | 81 | 14 | 50 |
| Cu | 98 | 34 | 266 | 84 | 226 |
| Zn | 124 | 48 | 323 | 109 | 246 |
| Cd | 1.0 | 0.1 | 3.7 | 0.7 | 2.4 |
| Ba | 85 | 14 | 158 | 91 | 145 |
| Hg | 6 | 0.07 | 138 | 1 | 4 |
| Pb | 27 | 9 | 90 | 20 | 66 |
| Mo | 7 | 3 | 19 | 5 | 17 |
| Si | 2642 | 1107 | 4387 | 3062 | 4249 |
| Zr | 2 | 0.7 | 5 | 2 | 4 |

For every site the highest concentration value was found for Si, followed by Fe, K, and Zn. Except for Zn, which in general has an anthropogenic origin, the other elements are often associated with a crustal origin [35,36].

Conversely, Co, Zr, and Cd have the lowest values in concentrations regardless of the investigated sites with Co and Zr that have a crustal origin whereas Cd is in general associated with anthropogenic sources [37].

Considering the only elements regulated in $PM_{10}$ Italian legislation and determined in this study (i.e., Cd, Ni, Pb), the mean concentrations for Cd and Pb are below the limit values for all the sites investigated (4 ng $m^{-3}$ for Cd, 0.5 μg $m^{-3}$ for Pb) while for Ni (20 ng $m^{-3}$) the average concentration is lower for Biella and Consolata sites and equal to the threshold value for Grassi site. Specifically, considering the values of Ni concentrations obtained in all the samples, we note that the threshold value has been exceeded in 2 out of

41 for Biella samples, 3 out of 33 for Consolata samples and 11 out of 33 for Grassi samples. The most overcomes occurred in November and December.

In general, the Biella site has the lowest average concentrations for all the analytes, except for V. This trend may be congruous considering how the site in question appears to be less polluted as shown by the monitoring studies carried out by ARPA. The exception of V may be due to an unidentified local source of this element that is characteristic of this site. No connection between the textile industry and V emission could be identified from the literature data, but mining, combustion of coals, utilization of petroleum and its products are the major anthropogenic sources of this element in the atmosphere [38,39].

The Grassi site appears to have higher concentrations than the Consolata site for the elements K, Ti, Cr, Mn, Fe, Ni, Cu, Zn, Cd, Ba, Hg, Pb, Mo, and Zr, which is consistent with the nature of the urban-industrial sampling site.

On the other hand, the Consolata site has the highest Si concentrations. In this station, which is subject to vehicular traffic, there are probably local uplifts of dust and soil, already shown in another study of this area [40].

In Table 5, there is a comparison of the concentrations of the elements determined in this study with other studies carried out on $PM_{10}$ in urban sites in Italian cities in the first decade of the 2000s [41–43] and with a study also carried out in the city of Turin in 2011 [40].

**Table 5.** Comparison of average element (expressed in ng $m^{-3}$) and $PM_{10}$ (expressed in μg $m^{-3}$) concentrations in different Italian towns.

| | Turin [1] | Turin [2] | Milan [3] | Rome [4] | Palermo [5] |
|---|---|---|---|---|---|
| K | 751 | 441 | 480 | | |
| Ti | 27 | 25 | 63 | 10 | |
| V | 5 | 3 | 9 | 3 | 22 |
| Cr | 13 | 10 | 14 | 7 | 9 |
| Mn | 29 | 23 | 35 | 10 | 18 |
| Fe | 1754 | 1902 | 1835 | 685 | 827 |
| Co | 0.7 | 0.7 | | | 0.3 |
| Ni | 18 | 6 | 10 | 4 | 8 |
| Cu | 86 | 45 | 68 | 38 | 83 |
| Zn | 107 | 74 | 213 | 70 | 60 |
| Cd | 0.9 | 0.9 | | 0.4 | |
| Ba | 63 | 62 | 92 | | 46 |
| Hg | 5 | 3 | | | |
| Pb | 24 | 15 | 215 | 16 | 17 |
| Mo | 6 | 5 | | | |
| Si | 3040 | | 4160 | 265 | |
| Zr | 2 | 2 | | | |
| $PM_{10}$ | 63 | 62 | 92 | | 46 |

[1] This study; [2] [40]; [3] [41]; [4] [42]; [5] [43].

The average $PM_{10}$ concentrations registered in Turin are in line with the national level. The concentrations of the elements determined in atmospheric particulate matter are also in the same order of magnitude. It is of interest to note that, according to Marcazzan et al. [41], the concentration of Pb is very high and this is because this metal was still permitted in gasoline fuels. After the phase-out of Pb from 2002 onwards, its concentration in atmospheric particulate matter decreased considerably [44].

An attempt was made to assess whether the elements determined in the $PM_{10}$ samples showed a seasonal trend and whether their trend varied between sites. To do this, the samples were divided according to month and the average concentration for each element was calculated according to site. August was excluded from the Biella samples because a comparison with the other two sites was not possible.

Figure 3 shows the seasonal trends for some of the elements determined, namely Si, K, V, Pb, and Mo. Regarding K, it is interesting to note that this element is more

abundant in November and December, especially for Consolata and Grassi sites, while this is less evident for the Biella site. K is an element that is generally used as a marker for biomass combustion, and this could explain why its concentration is higher precisely in the aforementioned months when the use of solid fuels for heating generation is higher [45,46].

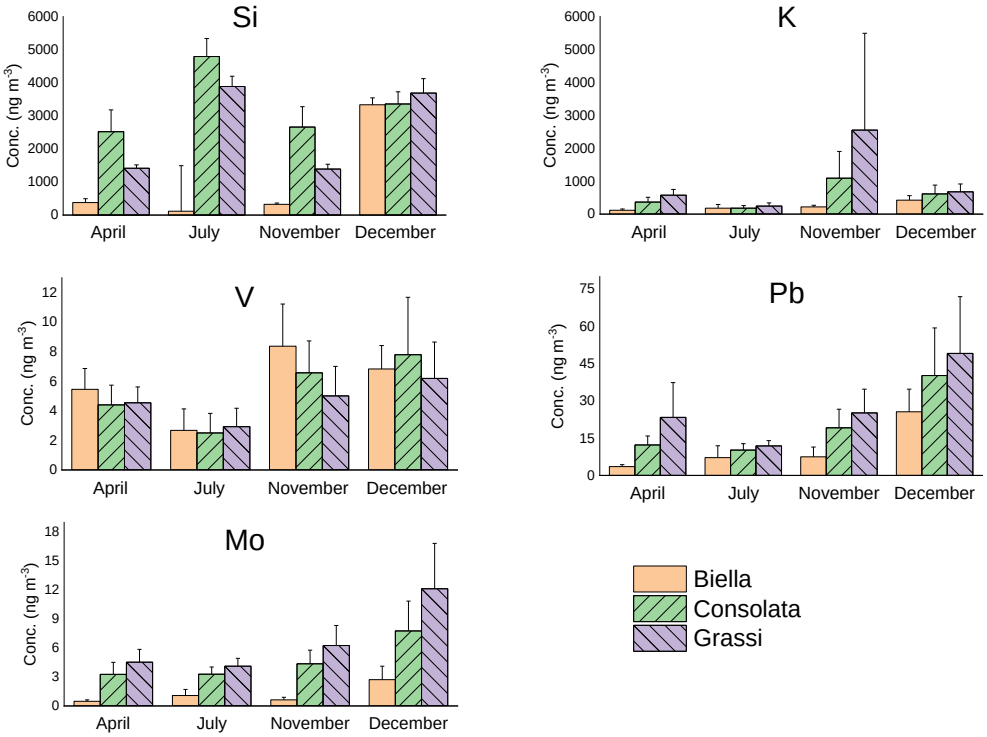


**Figure 3.** Concentrations of the elements Si, K, V, Pb, and Mo in ng $m^{-3}$ for Biella, Consolata, and Grassi sites according to the sampling month. The bars correspond to the positive standard deviation of the data.

Silicon is typically a crustal element, and high values of geogenic elements generally occur in the summer period. A very pronounced peak in the Si concentration has been recorded in July for each site. Moreover, there is a second peak for the month of December only for Biella and Grassi sites. Generally, Consolata site shows higher Si concentration than the other two sites for each considered month. This underlines how Si is characteristic for this site.

Regarding elements of probable anthropogenic origin, such as V, Pb, and Mo, it is possible to see that they are most abundant in November and December at the Consolata and Grassi sites and they have a minimum in July, in agreement with the characteristic seasonal trend of anthropogenic elements [40,47].

In contrast, the trends of these elements for the Biella site are peculiar. Pb and Mo appear to be more abundant in December, but November is comparable in concentration to July, which could suggest that this city is less polluted than Turin. As previously said, V is peculiar for Biella site, and stands out from the other two anthropogenic elements, showing a similar trend to the Consolata and Grassi sites but being more abundant in November than in December.

### *3.2. Crustal Enrichment Factors*

To establish the influence of the different emission sources on the concentrations of major, minor, and trace elements in $PM_{10}$ samples, crustal enrichment factors (CEF) were calculated for each site. This is a valid tool used in many studies concerning air pollution [48,49]. The aim is to assess if there is a difference in the origin of the elements between the different sites.

CEFs are calculated taking into account the average of Earth's upper crust composition values reported by Wedepohl et al. [50] to distinguish elements of pure geogenic origin from those that have been subjected to an enrichment by another source (typically anthropic). They were computed according to the following equation:

$$EF_i = \frac{\frac{C_i PM}{C_{Ti} PM}}{\frac{C_i crust}{C_{Ti} crust}} \quad (5)$$

where ($C_i PM/C_{Ti} PM$) is the concentration ratio between the $i$-th metal and Ti in the sample and ($C_i crust/C_{Ti} crust$) is the same concentration ratio in Earth's upper crust. We used Ti as a reference element since the soil is considered to be the major source of Ti in aerosol [51].

According to CEF values, it is possible to interpret the major categories of sources contributing to the metal contents in PM. CEF values less than 10 indicate that the element (defined as "unenriched") has predominantly a geogenic origin, whereas CEF values between 10 and 100 show that the element (defined as "moderately enriched") has a mixed origin and, finally, CEF values greater than 100 indicate that the element (defined as "enriched") has predominantly a non-geogenic origin. Figure 4a shows the CEFs obtained considering all the $PM_{10}$ samples grouped by sampling site. The results show that K, Mn, Fe, Si, and Zr have a purely crustal origin for all the sites investigated. In contrast, Cu, Zn, Cd, Mo, and Hg show a purely non-crustal origin in all the sites. They probably derive from anthropic sources, because they are usually associated to anthropic activity and the sampling sites can be considered located in industrial cities. For the Biella site, V and Cr show a mixed origin that probably includes an anthropogenic and crustal contribution. It is difficult to predict the origin of Co, Ba, Pb, and Ni, due to their positioning on the graph and the variability of their CEF values, which could indicate a different origin depending on the seasons. However, for Pb and Ni, the contribution of an anthropic source is evident.

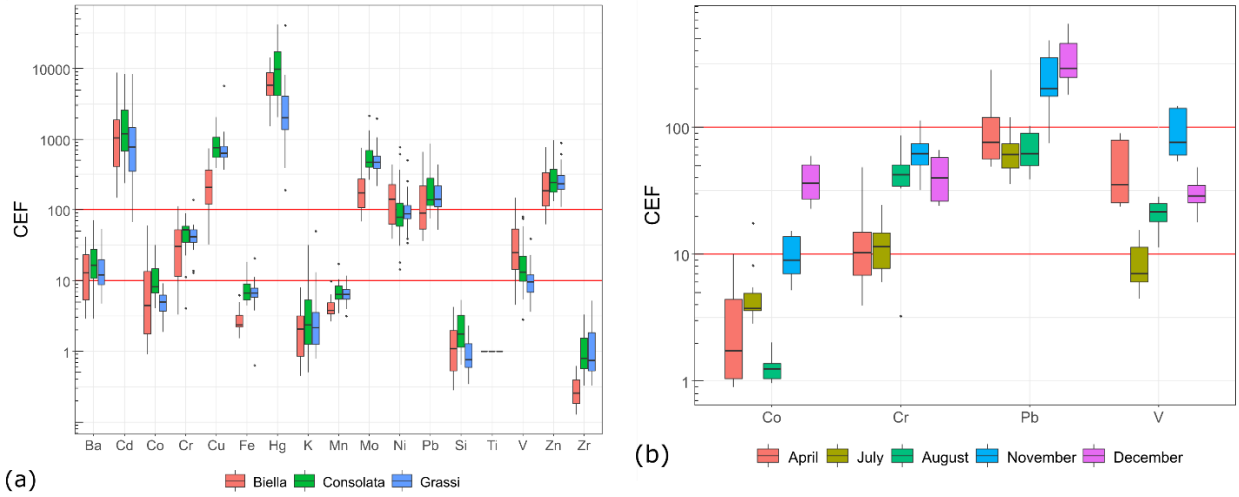


**Figure 4.** Crustal enrichment factors for $PM_{10}$ samples collected during 2007; (**a**) CEF values sorted according to the sampling site; (**b**) CEF values sorted according to the month of sampling for the samples collected at Biella site.

For the sampling site of Consolata, Cr, V, and Ba show a mixed origin, whereas Pb shows an anthropic origin. Co and Ni can be associated with multiple sources even if not so uniquely clear, and the reason could be attributed to the seasonal variability of their origin. For the Grassi site, we observed that Co and V seem to have a geogenic origin, partially in contrast with the results obtained with the other sites. Cr, Ni, and Ba show a mixed source and Pb confirms to be an element of mainly anthropic origin.

No significant difference was noted between the Consolata and Grassi sites. All elements exhibit monthly CEF values (not shown) comparable with those previously

shown. These results are in accordance with a similar investigation performed on $PM_{10}$ collected in Turin [40,52] and other industrialized cities [49,53].

As concerns the site of Biella, a significant variability between the CEF values of the different months can be noted for V, Cr, Co, and Pb (Figure 4b). Anthropogenic contribution seems to be predominant for Cr and Pb in August, November, and December compared to April and July. Differently, V shows higher CEF values in April and November, whereas Co has higher values in December. For this site, therefore, a greater variability in the emissive sources that influence the metal content in the $PM_{10}$ during the year is evident.

### *3.3. Chemometric Analysis*

The chemometric analysis uses a set of statistical techniques to extract the information contained in a multivariate dataset. Here, two of the most used techniques for the exploration of multivariate data, namely principal component analysis (PCA) and hierarchical clustering analysis (HCA), have been used to identify the possible sources of elements and to highlight spatial (between the sampling sites) and temporal (between the different months) differences [40,54]. Before the statistical treatments, the data were scaled for the mean value and normalized for the standard deviation (autoscaling). This approach has been used on the concentration expressed as the mass of the metals for the unit of air volume (ng $m^{-3}$) and as mass of metal for the unit of mass of $PM_{10}$ (mg $g^{-1}$).

Figure 5 shows the loading values for the first principal component (PC1), which describes almost 56% of the total variance of the data. As can be seen, all variables have positive loadings: therefore, PC1 can be considered as a new cumulative index to describe the level of contaminants in air. However, it is possible to discriminate two groups of variables according to their loading values, that is, according to the influence that each variable has on the definition of the new index. The first group contains Zr, Co, Ba, Ti, Cu, Pb, Cr, Zn, Mn, Fe, Mo, and the mass concentration of $PM_{10}$, and the second one contains the variables that less affect this component (Hg, Ni, Cd, Si, K, and V).

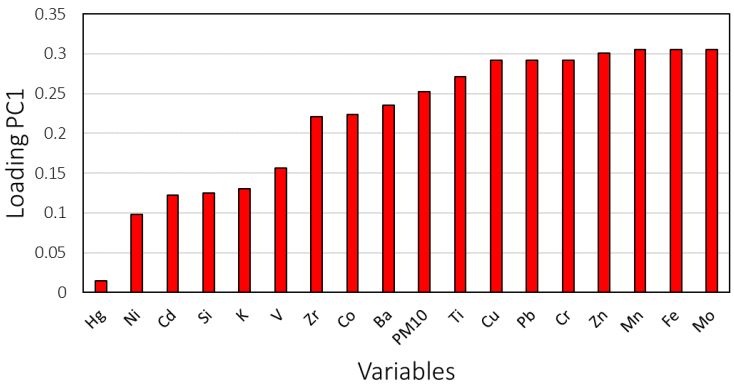


**Figure 5.** Loading values for PC1. The original data are expressed as metals mass amounts per unit of volume of air (ng $m^{-3}$).

From the box plots of the scores of the samples on PC1 (Figure 6) it is possible to notice that there is a statistical difference (*t*-test, *p*-value < 0.001) between the samples collected in Turin (pooling samples from Consolata and Grassi) and Biella. In fact, more than 60% of the samples from Turin have positive score values, while the samples from Biella have almost all negative scores. This difference highlights a higher content of $PM_{10}$ and higher metal concentrations in the samples from Turin. A difference between the samples of Consolata and Grassi is also observed, even if it is less statistically significant (*t*-test, *p*-value = 0.03). Regarding the seasonal differences, from the PCA, it emerges that only the samples collected in December are significantly different from the others (*t*-test, *p*-value < 0.01), having almost 88% of the score values on PC1 positive, against the 30%, 27%, and 38% for April, July, and November samples, respectively. Although the month of February possesses positive scores, and its position may be justified as a winter month,

its numerosity is too low to be compared with the other months. For the same reason, the samples collected during this month were not taken into account in the discussion of chemometric results. Again, the samples collected in December were those with higher $PM_{10}$ and metal concentrations.

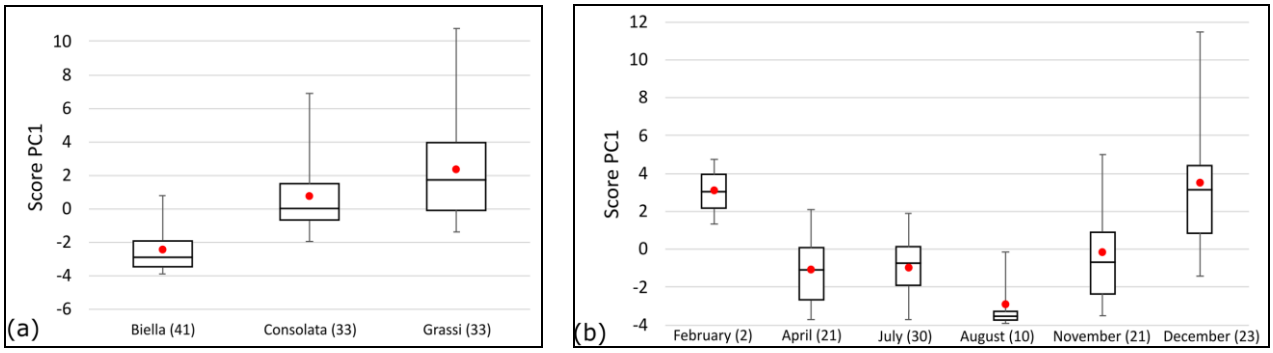


**Figure 6.** Boxplot of the score values of samples on PC1 considering (**a**) the samples sorted by the site of sampling, and (**b**) the month of sampling. The numerosity of each cluster is reported in round brackets.

HCA can be used to confirm the groups of variables that have previously been recognized by PCA, as well as to organize the samples by their similitudes. Differently from PCA, HCA considers all the information brought by the dataset. The dendrogram in Figure S1, obtained by R-mode cluster analysis, shows the three clusters recognized by the Hartigan index method. One of these contains almost all the samples from Biella. This is the set of less polluted samples. A second cluster contains the samples from Turin (Grassi and Consolata) and those from Biella of December. Finally, the samples from Grassi and Consolata collected in December split from the others at a high level of dissimilarity. These samples are the most polluted. Therefore, it is evident that the most polluted samples of Biella were similar to the less polluted samples from Turin.

So far, the concentration of the metals as the mass of elements per volume of air has been considered. However, this way to express the data does not consider the variation of the composition of PM, i.e., the variability of the ratio between its constituents. To evaluate this aspect, the concentration of metals per unit of mass of particulate (mg $g^{-1}$) has been now considered. As previously done, PCA and HCA were performed to evaluate the seasonal variability and the differences between the sampling sites. The evaluation of the scree plot shows that the first two components (PC1 and PC2) describe 61% of the total variance of the dataset and are sufficient to depict the samples correlation. The loading plot for the couple PC1-PC2 is reported in Figure 7a. These components group the variables in three clusters: Hg, K, Cd, Cr, Fe, Mo, Cu, and Zr at positive values of PC2; Ni, Si, Ti, Pb, Ba, Zn, and Mn at low-negative values of PC2. Finally, Co and V fall apart at high-negative values of PC2. All variables have positive values of PC1. Inside the groups mentioned above, it is possible to notice the strong correlation between Fe and Mo (Pearson coefficient 0.94, $p$-value < 0.0001), Cu (0.87, $p$-value < 0.0001), and Cr (0.86, $p$-value < 0.0001), suggesting a common origin linked to the emission from vehicular traffic and road dust. This emphasizes the double provenience for Fe (crustal and anthropic), also suggested by the lower correlation with Si (0.66, $p$-value < 0.0001), and previously highlighted by the crustal enrichment factors.

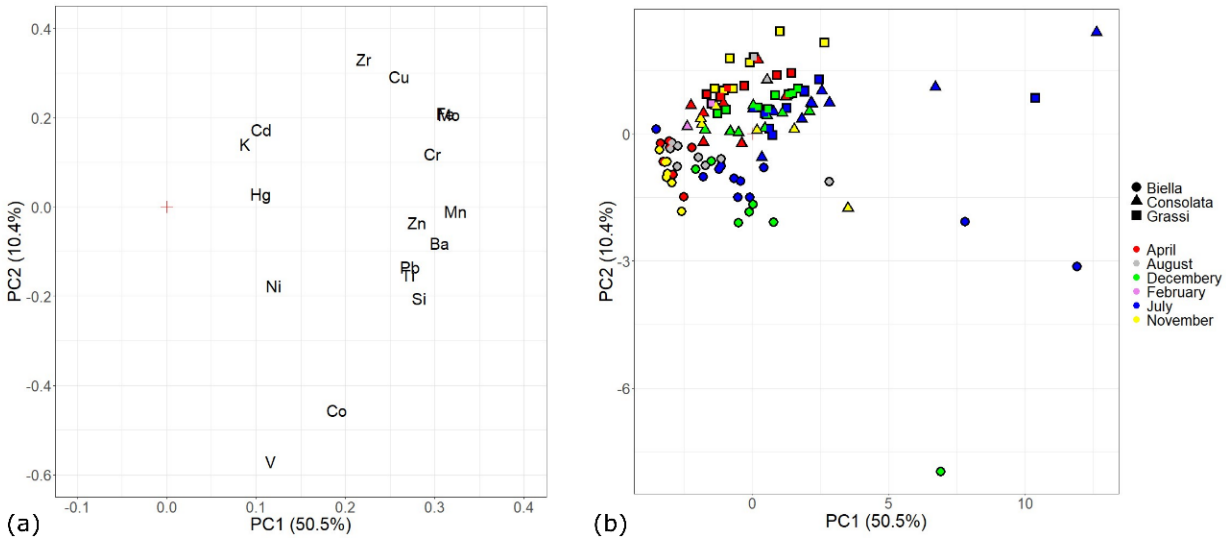


**Figure 7.** Loading and score plots for PC1 and PC2. The chemometric treatment was performed on data expressed as metals mass amounts per unit of mass of $PM_{10}$ (mg $g^{-1}$). (**a**) Loading plot; (**b**) Score plot.

The score plot in Figure 7b shows how the second principal component allows separating samples of Biella (negative scores) from those of Turin (positive scores). The latter are more affected by Fe, Mo, Cr, and Cu variables, which have positive loadings on PC2, while samples from Biella are most affected by Ni, Co, and V (especially some summer and autumn samples), which have negative loadings on PC2. Moreover, there is not a clear seasonality difference in the $PM_{10}$ composition. In fact, only a few samples of July from all sites fall apart from the cluster with others. These samples have a significantly different metal composition of $PM_{10}$, with enrichment of Mn, Zn, and Ba.

The cluster analysis performed on the variables (Q-mode analysis; Figure S2) recognizes two main clusters: the first one can be divided into three sub-clusters, one containing Si, Ti, and Mn, the second containing Cu, Fe, Mo, and the last with Zn, Cr, and Ba. In this cluster, crustal elements (e.g., Ti and Si) are mixed with anthropogenic ones (e.g., Cu and Zn). The second cluster contains Cd, Hg, K, Ni, V, Co, and Pb. All these elements can be connected to anthropic sources.

### *3.4. Risk Analysis*

The descriptive statistics for the *THQ* values for V, Cr, Mn, Co, Ni, and Cd, calculated as reported previously, for adults and children targets are reported in Table 6. The *THQ* values are quite lower than the threshold value of unity, except for Cd in children (4.679). Generally, the *THQ* values are higher for children than adults, according to the fact that children are more susceptible to these pollutants than adults. Significant differences have not been detected between the different months, while there were significant differences between the sampling sites ($p$-value < 0.01). In fact, the highest *THQ* values were found for the city of Turin, especially for Cr, Mn, and Cd (Figure 8). In this figure, the bars indicate the variability of the *THQ* values for each site (their length corresponds to the standard deviation).

Even if the air of Turin and Biella has a high amount of $PM_{10}$, the concentration of toxic metals is not so high as to induce concern about non-carcinogenic diseases by inhalation exposure, according to the USEPA exposure model. This result agrees with those reported for other urban districts [55–57].

**Table 6.** Descriptive statistics of *THQ* values for adults and children.

| | V | Cr | Mn | Co | Ni | Cd |
|---|---|---|---|---|---|---|
| | | | Adults | | | |
| Mean | 0.011 | 0.015 | 0.090 | 0.022 | 0.033 | 0.015 |
| Standard deviation | 0.006 | 0.014 | 0.076 | 0.021 | 0.052 | 0.015 |
| Median | 0.010 | 0.011 | 0.075 | 0.016 | 0.020 | 0.009 |
| 25% perc. | 0.007 | 0.005 | 0.032 | 0.007 | 0.012 | 0.005 |
| 75% perc. | 0.014 | 0.018 | 0.121 | 0.029 | 0.040 | 0.017 |
| IQR | 0.007 | 0.013 | 0.088 | 0.022 | 0.029 | 0.012 |
| Numerosity | 107 | 106 | 107 | 107 | 105 | 107 |
| | | | Children | | | |
| Mean | 0.038 | 0.054 | 0.327 | 0.078 | 0.122 | 4.679 |
| Standard deviation | 0.022 | 0.051 | 0.275 | 0.076 | 0.189 | 3.201 |
| Median | 0.035 | 0.039 | 0.274 | 0.056 | 0.072 | 4.872 |
| 25% perc. | 0.024 | 0.019 | 0.118 | 0.026 | 0.044 | 1.738 |
| 75% perc. | 0.050 | 0.066 | 0.439 | 0.105 | 0.148 | 7.252 |
| IQR | 0.026 | 0.047 | 0.321 | 0.079 | 0.104 | 5.514 |
| Numerosity | 107 | 106 | 107 | 107 | 105 | 107 |

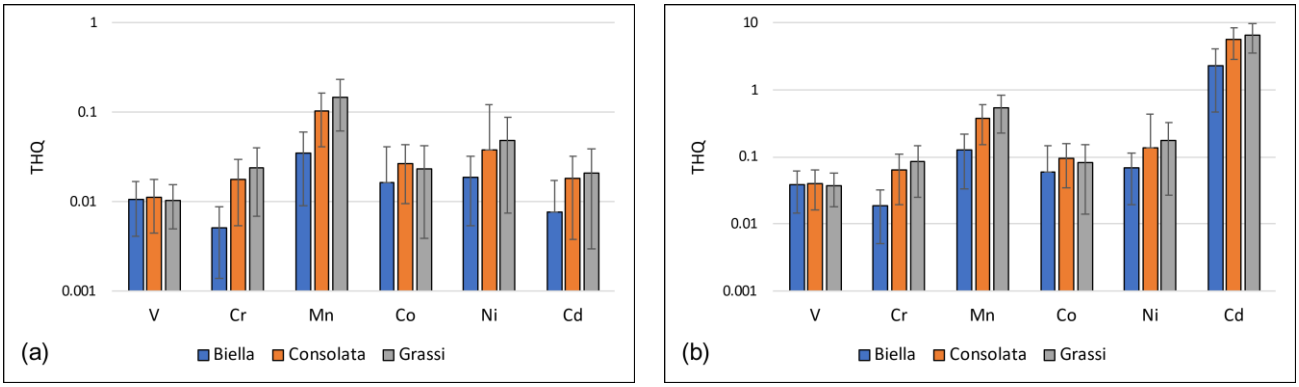


**Figure 8.** *THQ* mean values for (**a**) adults and (**b**) children for the site of Biella, Consolata, and Grassi. The length of the bars corresponds to the standard deviation of the data and represents the dispersion of the values.

### *3.5. Temporal Evolution*

ARPA Piedmont performs the monitoring of the air quality in many sites of the regional territory collecting the results in an open-access database (https://aria.ambiente.piemonte.it/#/qualita-aria/dati, accessed on 30 November 2022). Regarding heavy metals in $PM_{10}$, the monitoring activity follows the European directive 2004/17/EC focusing the attention on Pb, Ni, Cd, and As [12].

Using the ARPA's data, we have considered the monthly mean concentrations of Pb, Ni, and Cd for April, July, August, November, and December for the years 2007, 2009, 2012, 2015, 2017, 2019, and 2021. The sampling sites considered were those of Consolata and Grassi, in Turin, and a pooled site for Biella. The latter is obtained by the mean of the metal concentrations in two quite close sampling sites, Sturzo and Lamarmora. The choice of the elements and the months considered have been driven by the available $PM_{10}$ samples and by analytes which had been analyzed. The goal was to highlight the variation of these pollutants, which are strictly connected to anthropic activities, in the $PM_{10}$ collected in these two industrial cities. Considering the differences in the concentrations between the 2007 and 2021, the data reveal that there was a significant diminution in the concentration of pollutants in both cities over the last 14 years (Figure 9 and Figure S3). The differences between the two years are statistically significant for each element and site (One-Way ANOVA, $p$-value < 0.1). However, some differences between the sampling sites emerged.

The station of Grassi (Turin) shows the lowest reduction in the annual mean concentrations: 69%, 67%, and 57% for Ni, Cd, and Pb, respectively. For the sampling site of Consolata, the corresponding figures are 78%, 80%, and 86%. These differences can be due to the different urban contexts of the two sites, since Consolata is in a residential zone, and Grassi is more subjected to vehicular/industrial emissions. Therefore, the effect of the regulations on the environment and health protection promoted in the last years have probably had less impact on the peripherical zone of the city of Turin where the sampling site Grassi is placed. The highest relative reduction was instead observed for Ni at Biella (92%). Instead, the reductions in the annual mean concentrations for Cd and Pb at Biella site were 69% and 74% respectively. This finding is in accordance with the greater decrease of the industrial park occurred in Biella compared to Turin over the last 14 years. The reduction of the concentration of Cd in the $PM_{10}$ is reflected in the reduction of the risk for children, who are more susceptible to its toxic effect (see above), due to inhalation exposure

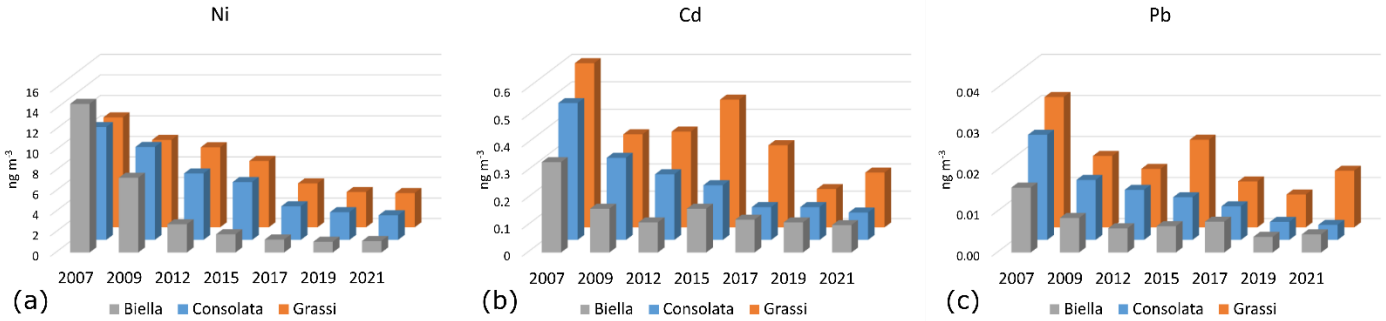


**Figure 9.** The trends of the mean concentration of (**a**) Ni, (**b**) Cd, and (**c**) Pb in $PM_{10}$ from Turin (Consolata, Grassi) and Biella from 2007 to 2021. Only the data of the months of April, July, August, November and December of each year have been considered. The data have been provided by ARPA Piedmont (https://aria.ambiente.piemonte.it/#/qualita-aria/dati; accessed on 30 November 2022).

Finally, in Figure S3, it is possible to notice a common seasonal variability in the concentrations for each site, with minimum values in July and August and maximum values during the winter and spring months.

## 4. Conclusions

The elemental characterization of the $PM_{10}$ of two industrial cities of North-West Italy, namely Turin and Biella, collected in 2007, has been performed to identify and characterize the emission sources affecting the air quality of these two cities.

$PM_{10}$ concentrations showed a clear seasonal trend with higher values in the cold months and lower values in the warm months for both cities considered. Concentrations of both $PM_{10}$ and elements determined were higher in Turin city, especially for the Grassi site which is confirmed to be a more polluted area compared with the other two under investigation.

From the use of crustal enrichment factors and the chemometric treatment performed, we can ascribe a probable crustal origin for the elements Si and Zr, and a probable anthropogenic origin for Cu, Zn, Cd, Mo, Ni, Pb, and Hg. Fe, Cr, Ba, K, V, Co, and Mn present an origin that may be due to a mixed anthropogenic and crustal contribution. The sites of Consolata and Biella appear to be characterized by a high concentration of Si and V, respectively.

Risk analysis was performed taking into account the amount of V, Cr, Mn, Co, Ni, and Cd. *THQ* values showed that only Cd was above the threshold value for children and in general the values for every element were higher for the city of Turin than Biella.

The analysis of the temporal evolution showed a decrease in the concentrations of the heavy metals Ni, Pb, and Cd over the period 2007–2021 with a reduction higher than 57% for all investigated sites.

This study shows how policies at national and European levels in recent years have contributed to a decrease in the concentration of metals in urban particulate matter, but in highly industrialized areas and in specific periods of the year, air quality is still an issue of primary concern for human health and the environment.

**Supplementary Materials:** The following supporting information can be downloaded at: https://www.mdpi.com/article/10.3390/atmos14010048/s1, Table S1: Instrumental technique used and principal information regarding the method of analysis, and the recovery obtained during the validation of the analytical method using the certified materials NIST SRM 1649a and BCR 176; Figure S1: Dendrogram for the HCA of the $PM_{10}$ samples (R-mode). The labels of the samples report the site of sampling (B for Biella, C for Consolata and G for Grassi) and are coloured as a function of the month: August (black), November (red), December (grenade), February (green), April (blue) and July (yellow); Figure S2: Dendrogram for HCA of the $PM_{10}$ samples for the variables (Q-mode). The data are expressed as metals mass amounts per unit of mass of $PM_{10}$ (mg $g^{-1}$); Figure S3: The trends of Ni, Cd, and Pb concentrations in $PM_{10}$ from Turin (Consolata, Grassi) and Biella from 2007 to 2021. The data have been provided by ARPA Piedmont (https://aria.ambiente.piemonte.it/#/qualita-aria/dati; accessed on 30 November 2022).

**Author Contributions:** Conceptualization, A.D., S.B. (Stefano Bertinetti), P.I. and M.M.; Formal analysis, A.D., S.B. (Stefano Bertinetti) and L.F.; Funding acquisition, M.M.; Investigation, A.D., S.B. (Stefano Bertinetti)and S.B. (Sandro Buoso); Methodology, O.A., A.G. and M.M.; Project administration, M.M.; Resources, O.A., A.G. and M.M.; Supervision, M.M.; Validation, S.B. (Sandro Buoso) and M.M.; Visualization, A.D., S.B. (Stefano Bertinetti) and S.B. (Sandro Buoso); Writing—original draft, A.D. and S.B. (Stefano Bertinetti); Writing—review & editing, A.D., S.B. (Stefano Bertinetti), O.A., L.F., P.I. and M.M. All authors have read and agreed to the published version of the manuscript.

**Funding:** This research received no external funding.

**Institutional Review Board Statement:** Not applicable.

**Informed Consent Statement:** Not applicable.

**Data Availability Statement:** Data are available upon request to the authors.

**Acknowledgments:** The authors want to thank the ARPA Piedmont for providing the samples and Andrea Sola and Luca Barletta for their help in the sample preparation and analysis.

**Conflicts of Interest:** The authors declare no conflict of interest. The funders had no role in the design of the study; in the collection, analyses, or interpretation of data; in the writing of the manuscript; or in the decision to publish the results.

## References

1. Moradi, M.; Mokhtari, A.; Mohammadi, M.J.; Hadei, M.; Vosoughi, M. Estimation of long-term and short-term health effects attributed to PM2.5 standard pollutants in the air of Ardabil (using Air Q + model). *Environ. Sci. Pollut. Res.* **2022**, *29*, 21508–21516. [CrossRef] [PubMed]
2. De Marco, A.; Amoatey, P.; Khaniabadi, Y.O.; Sicard, P.; Hopke, P.K. Mortality and morbidity for cardiopulmonary diseases attributed to PM2.5 exposure in the metropolis of Rome, Italy. *Eur. J. Intern. Med.* **2018**, *57*, 49–57. [CrossRef] [PubMed]
3. Conca, E.; Malandrino, M.; Giacomino, A.; Inaudi, P.; Giordano, A.; Ardini, F.; Traversi, R.; Abollino, O. Chemical fractionation of trace elements in arctic PM10 samples. *Atmosphere* **2022**, *12*, 1152. [CrossRef]
4. EEA (European Environment Agency). 2021 Europe's Air Quality Status 2021-Update; Web Report. Available online: https://www.eea.europa.eu/publications/air-quality-in-europe-2021/air-quality-status-briefing-2021 (accessed on 25 November 2022).
5. World Health Organization Europe. New WHO Global Air Quality Guidelines Aim to Save Millions of Lives from Air Pollution. 2021. Available online: https://www.who.int/news/item/22-09-2021-new-who-global-air-quality-guidelines-aim-to-save-millions-of-lives-from-air-pollution (accessed on 25 November 2022).
6. Tavella, R.A.; de Lima, B.R.; Ramires, P.F.; Santos, J.E.K.; Carvalho, R.B.; Marmett, B.; Vargas, V.M.F.; Baisch, P.R.M.; da Silva, J.F.M.R. Health impacts of PM2.5-bound metals and PAHs in a medium-sized Brazilian city. *Environ. Monit. Assess.* **2022**, *194*, 622. [CrossRef] [PubMed]
7. Galindo, N.; Yubero, E.; Nicolás, J.F.; Varea, M.; Crespo, J. Characterization of metals in PM1 and PM10 and health risk evaluation at an urban site in the western Mediterranean. *Chemosphere* **2018**, *201*, 243–250. [CrossRef]
8. Romanazzi, V.; Casazza, M.; Malandrino, M.; Maurino, V.; Piano, A.; Schilirò, T.; Gilli, G. PM10 Size Distribution of Metals and Environmental-Sanitary Risk Analysis in the City of Torino. *Chemosphere* **2014**, *112*, 210–216. [CrossRef]

9. Dockery, W.D.; Stone, P.H. Cardiovascular risks from fine particulate air pollution. *N. Engl. J. Med.* **2007**, *356*, 511–513. [CrossRef]
10. Zhang, J.X.; Zhou, Q.F.; Su, R.J.; Sun, Z.D.; Zhang, W.F.; Jin, X.T.; Zheng, Y.X. Cardiac dysfunction and metabolic remodeling due to seasonally ambient fine particles exposure. *Sci. Total Environ.* **2020**, *721*, 137792. [CrossRef]
11. Directive 2008/50/EC of the European Parliament and of the Council of 21 May 2008 on Ambient Air Quality and Cleaner Air for Europe. Available online: http://eur-lex.europa.eu/legal-content/en/ALL/?uri=CELEX:32008L0050 (accessed on 30 November 2022).
12. Directive 2004/107/EC of the European Parliament and of the Council of 15 December 2004 Relating to Arsenic, Cadmium, Mercury, Nickel and Polycyclic Aromatic Hydrocarbons in Ambient Air. Available online: https://eur-lex.europa.eu/legal-content/EN/TXT/?uri=CELEX%3A32004L0107 (accessed on 30 November 2022).
13. Dlgs 155, 2010. Attuazione Della Direttiva 2008/50/CE Relativa Alla Qualità Dell'aria Ambiente e per Un'aria Più Pulita in Europa. Official Gazette n. 216 of the Italian Republic. Available online: https://www.gazzettaufficiale.it/eli/id/2010/09/15/010G0177/sg (accessed on 30 November 2022).
14. Moreda-Pineiro, J.; Dans-Sanchez, L.; Sanchez-Pinero, J.; Turnes-Carou, I.; Muniategui-Lorenzo, S.; Lopez-Mahia, P. Oral bioavailability estimation of toxic and essential trace elements in PM10. *Atmos. Environ.* **2019**, *213*, 104–115. [CrossRef]
15. Fang, W.X.; Yang, Y.C.; Xu, Z.M. PM10 and PM2.5 and Health Risk Assessment for Heavy Metals in a Typical Factory for Cathode Ray Tube Television Recycling. *Environ. Sci. Technol.* **2019**, *47*, 12469–12476. [CrossRef]
16. Raffaelli, K.; Deserti, M.; Stortini, M.; Amorati, R.; Vasconi, M.; Giovannini, G. Improving air quality in the Po Valley, Italy: Some results by the LIFE-IPPREPAIR Project. *Atmosphere* **2020**, *11*, 429. [CrossRef]
17. Carugno, M.; Consonni, D.; Randi, R.; Catelan, D.; Grisotto, L.; Bertazzi, P.A.; Biggeri, A.; Baccini, M. Air Pollution Exposure, Cause-Specific Deaths and Hospitalizations in a Highly Polluted Italian Region. *Environ. Res.* **2016**, *147*, 415–424. [CrossRef] [PubMed]
18. Eurostat Statistics Explained 2022, Passenger Cars in the EU. 2022. Available online: https://ec.europa.eu/eurostat/statistics-explained/index.php?title=Passenger_cars_in_the_EU#Overview:_car_numbers_grow_with_a_rapid_increase_in_electric_but_a_low_share_of_overall_alternative_fuels (accessed on 25 November 2022).
19. Malandrino, M.; Casazza, M.; Abollino, O.; Minero, C.; Maurino, V. Size Resolved Metal Distribution in the PM Matter of the City of Turin (Italy). *Chemosphere* **2016**, *147*, 477–489. [CrossRef]
20. ARPA Piemonte Relazione Annuale Sui Dati Rilevati Dalla Rete Provinciale Di Monitoraggio Della Qualità Dell'aria. Anno 2007. Uno Sguardo All'aria. 10 Anni Dopo. 2007, p. 162. Available online: http://www.cittametropolitana.torino.it/cms/risorse/ambiente/dwd/qualita-aria/relazioni-annuali/relazione2007.pdf (accessed on 30 November 2022).
21. Bro, R.; Smilde, A.K. Principal Component Analysis. *Anal. Methods* **2014**, *6*, 2812–2831. [CrossRef]
22. Govender, P.; Sivakumar, V. Application of K-Means and Hierarchical Clustering Techniques for Analysis of Air Pollution: A Review (1980–2019). *Atmos. Pollut. Res.* **2020**, *11*, 40–56. [CrossRef]
23. R Core Team. R: A Language and Environment for Statistical Computing. R Foundation for Statistical Computing: Vienna, Austria, 2020; Available online: http://www.r-project.org/index.html (accessed on 30 November 2022).
24. Leardi, R.; Melzi, C.; Polotti, G. CAT (Chemometric Agile Tool). Available online: http://www.gruppochemiometria.it/index.php/software/19-download-the-r-based-chemometric-software (accessed on 14 December 2022).
25. de Vries, A.; Ripley, B.D. Ggdendro: Create Dendrograms and Tree Diagrams Using "Ggplot2". Available online: https://rdrr.io/bioc/structToolbox/man/hca_dendrogram.html (accessed on 30 November 2022).
26. Galili, T. Dendextend: An R Package for Visualizing, Adjusting and Comparing Trees of Hierarchical Clustering. *Bioinformatics* **2015**, *31*, 3718–3720. [CrossRef]
27. EPA Risk Assessment Guidance for Superfund. Volume I Human Health Evaluation Manual (Part A). 1989; Volume I, p. 289. Available online: https://www.epa.gov/risk/risk-assessment-guidance-superfund-rags-part (accessed on 30 November 2022).
28. United States Environmental Protection Agency (US-EPA) Risk Assessment Guidance for Superfund, Volume I: Human Health Evaluation Manual, Supplemental Guidance for Standard Default Exposure Factors. Oswer Dir. 9285.6-03 2009, I. Available online: https://www.epa.gov/sites/default/files/2015-09/documents/rags_a.pdf (accessed on 30 November 2022).
29. U.S. EPA United States Environmental Protection Agency. *Exposure Factors Handbook 2011 Edition (Final Report)*; EPA/600/R-09/052F; U.S. Environmental Protection Agency: Washington, DC, USA, 2011.
30. Nidzgorska-Lencewicz, J.; Czarnecka, M. Thermal Inversion and Particulate Matter Concentration in Wrocław in Winter Season. *Atmosphere* **2020**, *11*, 1351. [CrossRef]
31. Largeron, Y.; Staquet, C. Persistent inversion dynamics and wintertime PM10 air pollution in Alpine valleys. *Atmos. Environ.* **2016**, *135*, 92–108. [CrossRef]
32. Ferrario, M.E.; Rossa, A.; Pernigotti, D. Characterization of PM10 Accumulation Periods in the Po Valley by Means of Boundary Layer Profilers. *IOP Conf. Ser. Earth Environ. Sci.* **2008**, *1*, 012067. [CrossRef]
33. Bigi, A.; Ghermandi, G. Climatology of Atmospheric PM10 Concentration in the Po Valley. Preprint. *Atmospheric Chem. Phys.* **2014**, *14*, 137–170. [CrossRef]
34. Prodi, F.; Belosi, F.; Contini, D.; Santachiara, G.; Di Matteo, L.; Gambaro, A.; Donateo, A.; Cesari, D. Aerosol Fine Fraction in the Venice Lagoon: Particle Composition and Sources. *Atmos. Res.* **2009**, *92*, 141–150. [CrossRef]
35. Sanderson, P.; Delgado-Saborit, J.M.; Harrison, R.M. A Review of Chemical and Physical Characterization of Atmospheric Metallic Nanoparticles. *Atmos Environ.* **2014**, *94*, 353–365. [CrossRef]

36. Rauch, J.N.; Pacyna, J.M. Earth's Global Ag, Al, Cr, Cu, Fe, Ni, Pb, and Zn Cycles: GLOBAL METAL CYCLES. *Glob. Biogeochem.* **2009**, *23*, GB2001. [CrossRef]
37. Pacyna, E.G.; Pacyna, J.M.; Fudala, J.; Strzelecka-Jastrzab, E.; Hlawiczka, S.; Panasiuk, D.; Nitter, S.; Pregger, T.; Pfeiffer, H.; Friedrich, R. Current and Future Emissions of Selected Heavy Metals to the Atmosphere from Anthropogenic Sources in Europe. *Atmos. Environ.* **2007**, *41*, 8557–8566. [CrossRef]
38. Schlesinger, W.H.; Klein, E.H.; Vengosh, A. Global Biogeochemical Cycle of Vanadium. *Proc. Natl. Acad. Sci. USA* **2017**, *114*, E11092–E11100. [CrossRef]
39. Hope, B.K. An Assessment of the Global Impact of Anthropogenic Vanadium. *Biogeochemistry* **1994**, *37*, 1–13. [CrossRef]
40. Padoan, E.; Malandrino, M.; Giacomino, A.; Grosa, M.M.; Lollobrigida, F.; Martini, S.; Abollino, O. Spatial distribution and potential sources of trace elements in PM10 monitored in urban and rural sites of Piedmont Region. *Chemosphere* **2016**, *145*, 495–507. [CrossRef]
41. Marcazzan, G.M.; Vaccaro, S.; Valli, G.; Vecchi, R. Characterisation of PM10 and PM2.5 Particulate Matter in the Ambient Air of Milan (Italy). *Atmos. Environ.* **2001**, *35*, 4639–4650. [CrossRef]
42. Astolfi, M.L.; Canepari, S.; Cardarelli, E.; Ghighi, S.; Marzo, M.L. Chemical Fractionation of Elements in Airborne Particulate Matter: Primary Results on PM10 and PM2.5 Samples in the Lazio Region (Central Italy). *Ann. Chim.* **2006**, *96*, 183–194. [CrossRef]
43. Dongarrà, G.; Manno, E.; Varrica, D.; Vultaggio, M. Mass Levels, Crustal Component and Trace Elements in PM10 in Palermo, Italy. *Atmos Environ.* **2007**, *41*, 7977–7986. [CrossRef]
44. Vestreng, V.; Breivik, K.; Adams, M.; Wagner, A.; Goodwin, J.; Rozovskaya, O.; Pacyna, J.M. Inventory Review 2005. Emission Data Reported to LRTAP Convention and NEC Directive. Initial Review for HMs and POPs. Oslo, Meteorological Synthesizing Centre—West (EMEP MSC-W Technical Report 1/2005). Available online: http://www.emep.int/publ/reports/2005/emep_technical_1_2005.pdf (accessed on 30 November 2022).
45. Andreae, M.O.; Merlet, P. Emission of trace gases and aerosols from biomass burning. *Glob. Biogeochem.* **2001**, *15*, 955–966. [CrossRef]
46. Caseiro, A.; Bauer, H.; Schmidl, C.; Pio, C.A.; Puxbaum, H. Wood burning impact on PM10 in three Austrian regions. *Atmos. Environ.* **2009**, *43*, 2186–2195. [CrossRef]
47. Cesari, D.; De Benedetto, G.E.; Bonasoni, P.; Busetto, M.; Dinoi, A.; Merico, E.; Chirizzi, D.; Cristofanelli, P.; Donateo, A.; Grasso, F.M.; et al. Seasonal Variability of PM2.5 and PM10 Composition and Sources in an Urban Background Site in Southern Italy. *Sci. Total Environ.* **2018**, *612*, 202–213. [CrossRef]
48. Megido, L.; Negral, L.; Castrillón, L.; Suárez-Peña, B.; Fernández-Nava, Y.; Marañón, E. Enrichment Factors to Assess the Anthropogenic Influence on PM10 in Gijón (Spain). *Environ. Sci. Pollut. Res.* **2017**, *24*, 711–724. [CrossRef]
49. Gharaibeh, A.A.; El-Rjoob, A.O.; Harb, M.K. Determination of Selected Heavy Metals in Air Samples from the Northern Part of Jordan. *Environ. Monit. Assess.* **2010**, *160*, 425–429. [CrossRef]
50. Wedepohl, K.H. The Composition of the Continental Crust. *Geochim. Et Cosmochim. Acta* **1995**, *59*, 1217–1232. [CrossRef]
51. Lawson, D.R.; Winchester, J.W. A standard crustal aerosol as a reference for elemental enrichment factors. *Atmos. Environ.* **1967**, *13*, 925–930. [CrossRef]
52. Malandrino, M.; Di Martino, M.; Giacomino, A.; Geobaldo, F.; Berto, S.; Grosa, M.M.; Abollino, O. Temporal Trends of Elements in Turin (Italy) Atmospheric Particulate Matter from 1976 to 2001. *Chemosphere* **2013**, *90*, 2578–2588. [CrossRef]
53. Toledo, V.E.; Almeida, P.B.; Quiterio, S.L.; Arbilla, G.; Moreira, A.; Escaleira, V.; Moreira, J.C. Evaluation of Levels, Sources and Distribution of Toxic Elements in PM10 in a Suburban Industrial Region, Rio de Janeiro, Brazil. *Environ. Monit. Assess.* **2008**, *139*, 49–59. [CrossRef]
54. Chavent, M.; Guégan, H.; Kuentz, V.; Patouille, B.; Saracco, J. PCA- and PMF-Based Methodology for Air Pollution Sources Identification and Apportionment. *Environmetrics* **2009**, *20*, 928–942. [CrossRef]
55. Negral, L.; Suarez-Pena, B.; Zapico, E.; Fernandez-Nava, Y.; Megido, L.; Moreno, J.; Maranon, E.; Castrillon, L. Anthropogenic and Meteorological in Fl Uences on PM10 Metal/Semi-Metal Concentrations: Implications for Human Health. *Chemosphere* **2020**, *243*, 125347. [CrossRef] [PubMed]
56. Brown, A.; Barrrett, J.E.S.; Robinson, H.; Potgieter-Vermaak, S. Risk Assessment of Exposure to Particulate Output of a Demolition Site. *Environ. Geochem. Health* **2015**, *37*, 675–687. [CrossRef]
57. Lu, X.; Wu, X.; Wang, Y.; Chen, H.; Gao, P.; Fu, Y. Risk Assessment of Toxic Metals in Street Dust from a Medium-Sized Industrial City of China. *Ecotoxicol. Environ. Saf.* **2014**, *106*, 154–163. [CrossRef]

# Supplementary Materials:

# $PM_{10}$ Element Distribution and Environmental-Sanitary Risk Analysis in Two Italian Industrial Cities

**Aleandro Diana [1], Stefano Bertinetti [1,*], Ornella Abollino [2], Agnese Giacomino [2], Sandro Buoso [1], Laura Favilli [2], Paolo Inaudi [2] and Mery Malandrino [1,*]**

[1] Department of Chemistry, University of Turin, 10125 Turin, Italy
[2] Department of Drug Science and Technology, University of Turin, 10125 Turin, Italy
* Correspondence: stefano.bertinetti@unito.it (S.B.); mery.malandrino@unito.it (M.M.)

**Table S1.** Instrumental technique used and principal information regarding the method of analysis, and the recovery obtained during the validation of the analytical method using the certified materials NIST SRM 1649a and BCR 176.

| Element | Instrumental Technique | Isotope/Wavelength | Resolution | Internal standard | Recovery (%) |
|---|---|---|---|---|---|
| **Ba** | ICP-MS | 135/137/138 | LR | Te 128 | 89.6 |
| **Cd** | ICP-MS | 113 | MR | Te 125 | 101.2 |
| **Co** | ICP-MS | 59 | LR | Te 128 | 79.5 |
| **Cr** | ICP-MS | 52 | MR | Te 125 | 51.7 |
| **Cu** | ICP-MS | 65 | MR | Te 128 | 89.9 |
| **Fe** | ICP-AES | *259.939 nm* | | | 86.3 |
| **Hg** | ICP-MS | 199/200/201 | LR | Te 125 | 90.9 |
| **K** | ICP-AES | *769.896 nm* | | | 116.0 |
| **Mn** | ICP-MS | 55 | MR | Te 125 | 77.6 |
| **Mo** | ICP-MS | 95/96 | LR | Te 128 | - |
| **Ni** | ICP-MS | 58 | LR | / | 96.3 |
| **Pb** | ICP-MS | 206 | LR | Te 125 | 100.9 |
| **Si** | ICP-MS | 28 | MR | Te 125 | - |
| **Ti** | ICP-AES | *334.940 nm* | | | 72.5 |
| **V** | ICP-MS | 51 | MR | Te 128 | 86.4 |
| **Zn** | ICP-MS | 64/66 | MR | Te 128 | 94.6 |
| **Zr** | ICP-MS | 90/91 | MR | Te 125 | - |

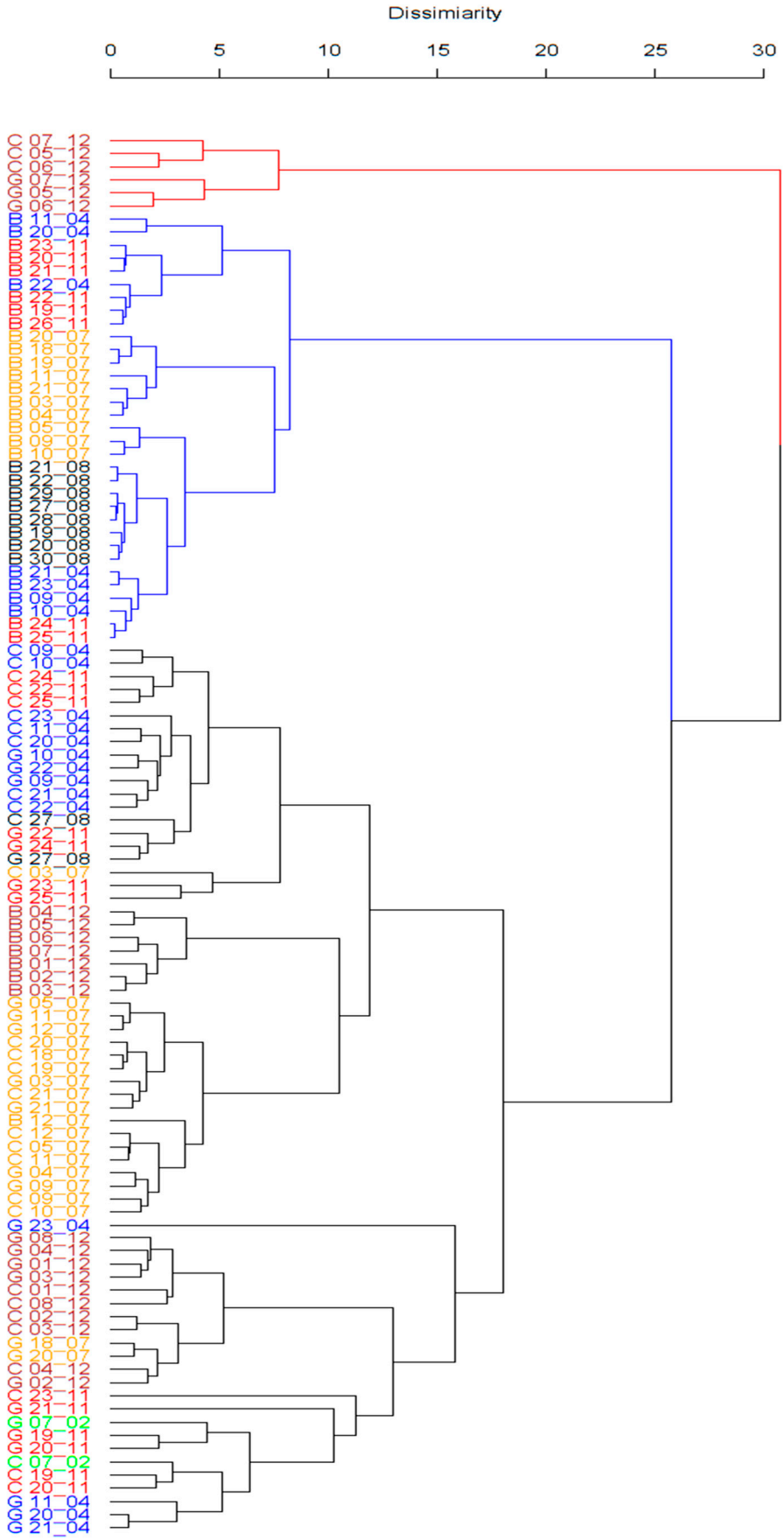


**Figure S1.** Dendrogram for the HCA of the $PM_{10}$ samples (R-mode). The labels of the samples report the site of sampling (B for Biella, C for Consolata and G for Grassi) and are coloured as a function of the month: August (black), November (red), December (grenade), February (green), April (blue) and July (yellow).

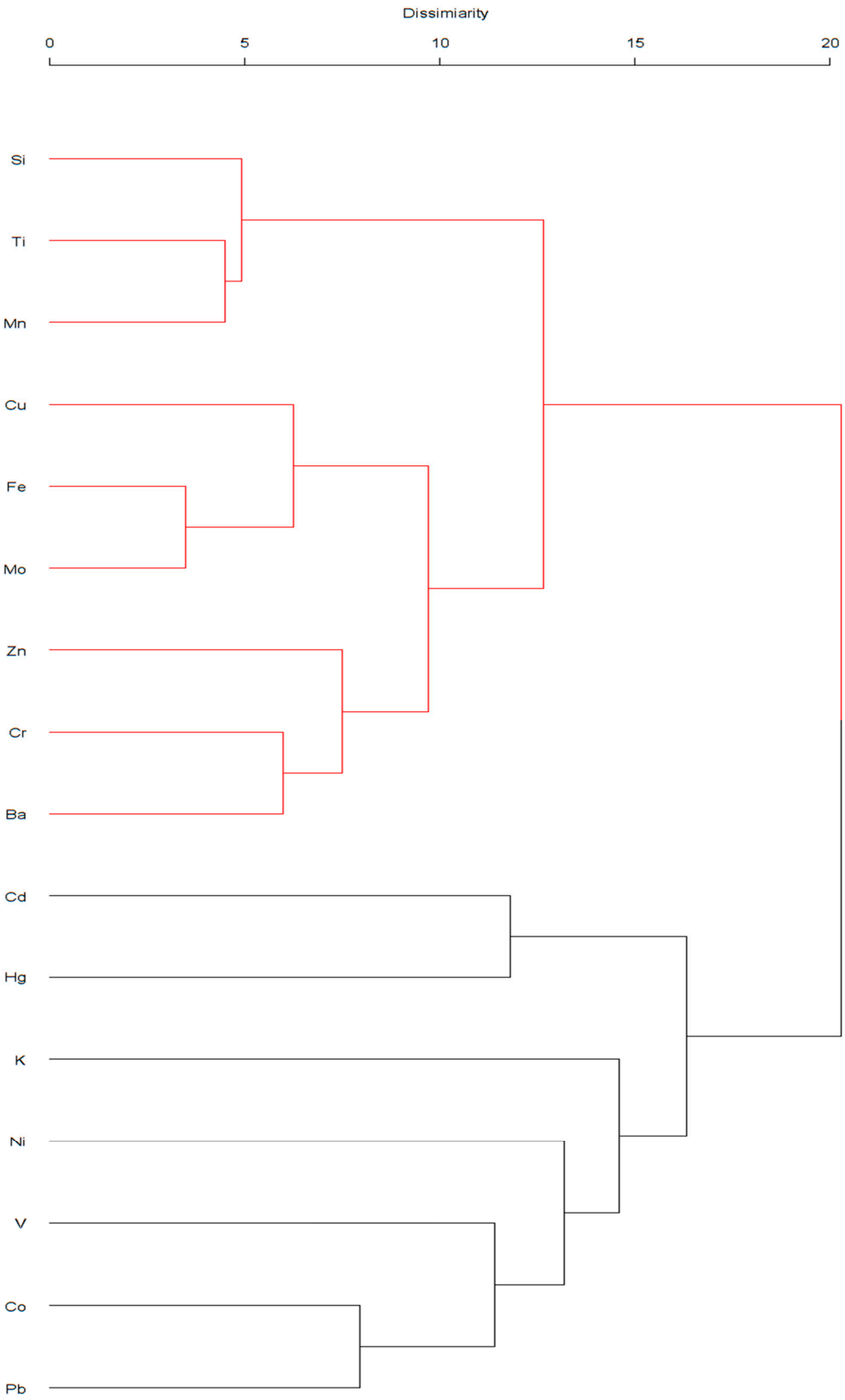


**Figure S2**. Dendrogram for HCA of the $PM_{10}$ samples for the variables (Q-mode). The data are expressed as metals mass amounts per unit of mass of $PM_{10}$ (mg $g^{-1}$).

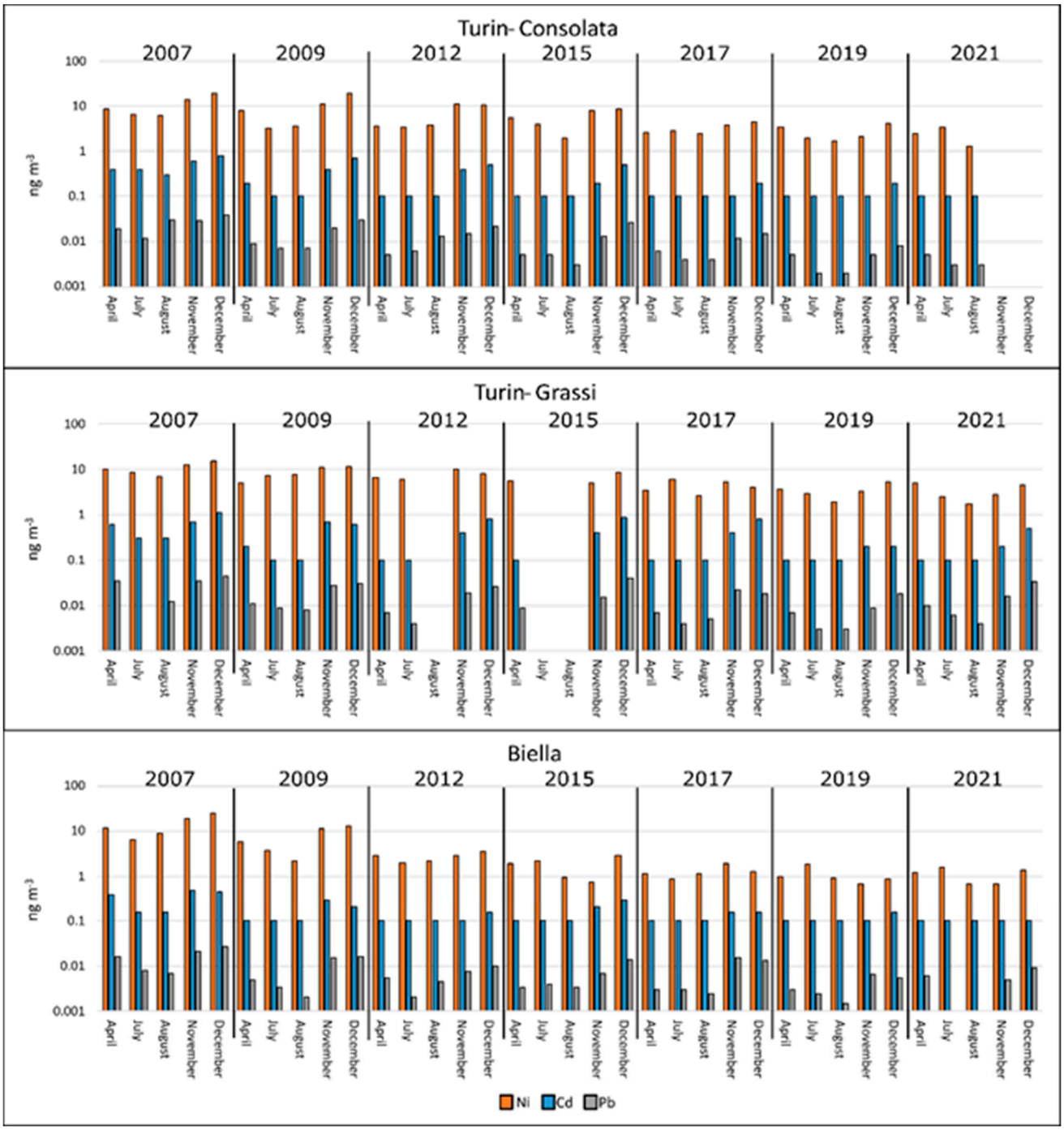


**Figure S3.** The trends of Ni, Cd, and Pb concentrations in PM10 from Turin (Consolata, Grassi) and Biella from 2007 to 2021. The data have been provided by ARPA Piedmont (https://aria.ambiente.piemonte.it/#/qualita-aria/dati).